J Electroceram (2011) 27:7–12
DOI 10.1007/s10832-010-9604-9

IR-wavelength optical shutter based on ITO/VO_2/ITO thin film stack

Santtu T. Heinilehto · Jyrki H. Lappalainen ·
Heli M. Jantunen · Vilho Lantto

Received: 19 September 2008 / Accepted: 4 April 2010 / Published online: 16 April 2010

Abstract Two thin film IR-shutter structures based on ITO-VO_2-ITO and ITO-VO_2 thin film stacks were designed. Thin film structures of the shutters were optimized at the wavelength of 1550 nm. The switch operation of the components was based on the metal-insulator transition phenomenon of VO_2. Shutter components were current controlled and the metal-insulator transition was induced by Joule heating effect. All the thin films were deposited by using pulsed laser deposition. Crystal structure, morphology, and optical characteristics of the produced components were studied. Components with three-layer structure were found to suffer from significant internal strain, which was relaxed by post-annealing the components in the furnace. The maximum change of the optical transmittance measured at the wavelength of 1550 nm from the three-layer components during the switch cycle was 26.5%. The corresponding value measured from two-layer component's structure was 34.2%. The maximum modulation of the transmittance of the three-layer component was reached at the wavelength of 1250 nm, which was 34%.

Keywords Vanadium dioxide · Metal-insulator transition · PLD

1 Introduction

Metal-insulator transition (MIT) is a physical phenomenon where material undergoes a transition from the insulating or semiconducting state to the conducting metallic state. Vanadium dioxide (VO_2) is a ceramic material which is known to undergo an abrupt MIT at the temperature of 68°C [1]. The MIT of VO_2 originates from the first order phase transition, where crystal structure of vanadium dioxide changes from monoclinic to tetragonal symmetry. During the phase transition atoms of the crystal structure reorganise, which causes changes in the energy band structure of the VO_2. Because of this, the Fermi-level of the VO_2 is placed inside the conduction band, which eventually causes the conductivity of VO_2 to increase by six orders of magnitude [2]. Vanadium dioxide is also a thermochromic material and thus the optical properties of VO_2 are significantly changed in the IR-region of the optical spectrum during the MIT [3, 4]. Because the transition temperature of vanadium dioxide is close to room temperature and both optical and electrical properties of the material are significantly changed when the MIT effect takes place, it is a suitable material for many electrical and optoelectrical applications, such as electrical and optical switches [5, 6], tunable photonic crystals [7], and thermal imaging sensors [8]. Recently, vanadium dioxide has been an intensively studied MIT material and VO_2 thin films have been deposited by using various thin film deposition methods, like e-beam evaporation [9], sputtering [10], pulsed laser deposition (PLD) [11, 12], and sol-gel [13].

Indium-tin oxide (ITO) is a transparent conductive oxide (TCO) material, which is optically transparent in the wavelengths ranging from the visible to near-infrared (NIR) area of the optical spectrum [14]. Also, ITO is a

---

S. T. Heinilehto (✉) · J. H. Lappalainen · H. M. Jantunen ·
V. Lantto
Microelectronics and Materials Physics Laboratories,
EMPART Research Group of Infotech Oulu,
University of Oulu,
P.O. Box 4500, Oulu FIN-90014, Finland
e-mail: santtu.heinilehto@ee.oulu.fi

widely studied material and it is broadly used in various optical applications, like liquid crystal displays. Several thin film deposition methods have also been demonstrated for ITO thin film production [15, 16].

In this paper, the use of VO_2thin films as a functional material for infrared wavelength optical shutter application is presented. Two different component structures were designed and their structural and optical characteristics were studied. The first component design was based on a three-layer thin film stack, where vanadium dioxide thin film was deposited between two ITO films, which worked as top and bottom electrodes. In another design the top ITO electrode was excluded and the component had a two-layer structure. Also, unoptimized shutter components were produced to test the material growth parameters. They were used for comparison to the performance of the other components. In all designs, operation of the component was based on the metal-insulator transition of VO_2 which was triggered by the Joule heating effect caused by current running through the VO_2 and ITO films. All the thin films were deposited by using the PLD method.

2 Experimental

Schematic pictures of the two IR-shutter component structures are presented in Fig. 1. In both designs, r-plane Al_2O_3 was selected as the substrate material for the thin film components because its high transparency at the wavelengths of the optical spectrum considered here.

The first component design presented in Fig. 1(a) was a multilayer structure with three layers. The bottom layer was an ITO film which worked as the bottom electrode of the structure. An active VO_2 film was deposited on top of the ITO bottom electrode. The topmost layer of the structure was another ITO film, which was deposited on top of the VO_2 thin film to work as the top electrode of the component. The structure was optimized at the wavelength of 1550 nm. The thicknesses of the films of the thin film stack were 520 nm for the bottom ITO electrode, 200 nm for the VO_2 layer, and 180 nm for the top ITO electrode. The other IR-shutter structure presented in Fig. 1(b) was a two-layer structure. It only had a bottom electrode ITO layer and VO_2 thin film deposited on top of it. The optimized thicknesses of the films at the wavelength of 1550 nm were 240 nm for the bottom electrode and 290 nm for the VO_2 layer. Platinum bonding pads were deposited on the bottom and top ITO electrodes in the case of the first design and on the bottom ITO electrode and the VO_2 film on the other design to work as electrical contacts areas. Produced components were electrically connected to the printed circuit boards by using wire bonder and gold wire. Both of the component structures were designed to operate so that the optical signal to be controlled was directed perpendicularly through the thin film stack and sapphire substrate.

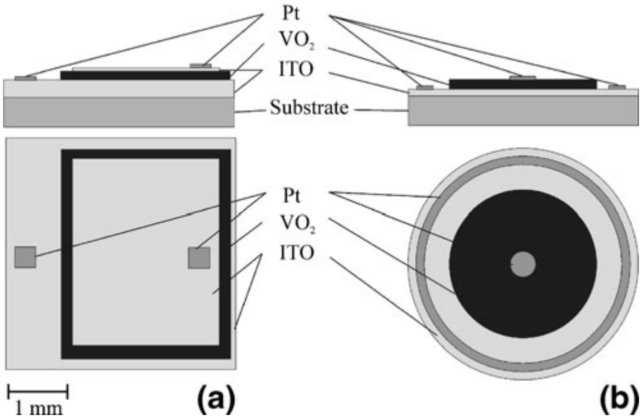

Fig. 1 Schematic presentation of the two IR-shutter component structures. (**a**) Three layer structure, dimensions of the films: bottom ITO electrode 4.2×4.2 mm, VO_2 film 3.8×3.3 mm, and top ITO electrode 3.4×2.9 mm. (**b**) Two layer structure, diameter of the films: bottom ITO electrode 5.6 mm and VO_2 film 3.6 mm. Rough lateral dimension scale bar presented

When voltage was applied between the electrical contacts, the current running through the ITO and VO_2 thin films caused heating of the VO_2 film through the Joule heating effect. This triggered the phase transition in the vanadium dioxide thin film and the MIT effect took place. When the transition from the semiconducting to conducting state took place, VO_2turned from optically transparent to opaque at IR-wavelengths and effectively blocked the IR-radiation. The shutter was thus in a closed state. When voltage was removed, the current reduced and the VO_2 film cooled down and was restored to its original open state.

All the thin films of the components were deposited by using PLD. The laser used in the deposition was a XeCl excimer laser operating at the wavelength of 308 nm and pulse duration of 25 ns. The pulse repetition rate was 5 Hz. The vacuum chamber was evacuated at the base pressure of 10^{-5}mbar and the temperature of the components during the deposition was 400°C. The laser beam fluence was 3 J/cm^2 for both ITO and VO_2 thin film depositions. Physical alumina masks were used to pattern the ceramic layers of the shutter components. In deposition of vanadium dioxide thin films, a pure ceramic vanadium pentoxide (V_2O_5) (SCI Engineered Materials, Inc.) target with a purity of 99.9% was used as a laser ablation target. Two different oxygen background pressures of 1.0×10^{-2}mbar and 1.3×10^{-2}mbar were used in VO_2 film depositions. ITO films were deposited by using an ITO target (90% In_2O_3-10% SnO_2) with a purity of 99.99%. The oxygen partial pressure inside the vacuum chamber during the ITO thin film deposition was 5.0×10^{-2} mbar. The platinum contact pads were produced by using the standard photolithographic process. Patterned photoresist was used as a mask for the electrode pad deposition. The

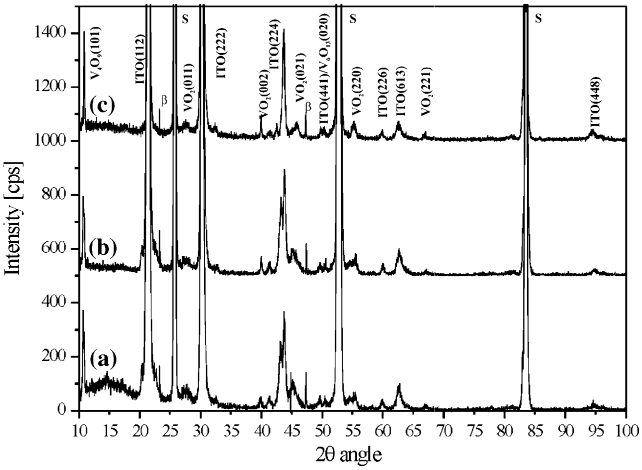

Fig. 2 XRD patterns measured from the three-layer shutter component with film thicknesses of 480 nm for bottom ITO electrode, 230 nm for VO_2 film, and 160 nm for top ITO electrode. The patterns are measured after deposition (**a**), after annealing the component 20 min at the temperature of 300°C in a N_2 atmosphere (**b**), and after annealing the component 20 min at the temperature of 450°C in a N_2 atmosphere (**c**). Substrate K_α and K_β reflections are labelled with S and β

target used in platinum film deposition was a pure metallic platinum target and the laser beam fluence was set to 14.3 J/cm^2. After the deposition, some of the samples were post-annealed for 20 min in a tube furnace in a pure N_2 atmosphere at temperatures of 300°C, 450°C and 500°C to relax the residual strain of the thin-film multilayer structure, which resists the phase transition of VO_2, and in this way enhances the optical response of the shutter components.

The crystal structure of the produced components was analyzed by using x-ray diffraction (XRD). θ-2θ measurements of the samples were performed by using a Philips PW1380 x-ray diffractometer. The surface structure of the components was studied by using a Veeco Nanoscope IV scanning probe microscope in contact mode atom force microscope (AFM) mode.

Characterization of the optical properties of the IR-shutter components was carried out by using Varian Cary 500 UV-vis-NIR spectrophotometer. Optical transmittance measurements were performed at the wavelength area between 175 and 2500 nm. The switch operation was induced by applying the potential difference over the thin film structure by connecting an Agilent E3614A dc power source between the top and bottom electrodes. The dynamic responses of the components were evaluated by using the computer-controlled Keithley 2612 SYSTEM SourceMeter as the ac voltage source. An IR-LED was selected as the optical signal source. The modulation of the optical signal during the switch cycle was recorded by using Thorlabs PDA50B photodetector which was connected to a digital oscilloscope.

3 Results and discussion

XRD patterns measured from the produced three-layer shutter components showed that the deposited thin films were clearly polycrystalline. All the deposited ITO films showed a film structure with (112) and (222) as their main crystal orientation, but also contained (213), (024), (224), (441), (145), (226), and (613) orientations. VO_2 films deposited with the oxygen partial pressures of 1.0×10^{-2} mbar and 1.3×10^{-2} mbar showed no significant difference in their crystal structure and were all polycrystalline films with (011), (002), (021), (220), and (221) crystal orientations. All the vanadium dioxide films also showed an indication of the presence of a small amount of other vanadium oxide phases in their crystal structure such as V_4O_9, V_6O_{13}, and V_2O_5.

Figure 2 shows three XRD patterns measured from the component with a three-layer structure. The lowest pattern in Fig. 2 was measured from the component after deposition, the pattern in the middle after annealing the sample 20 min

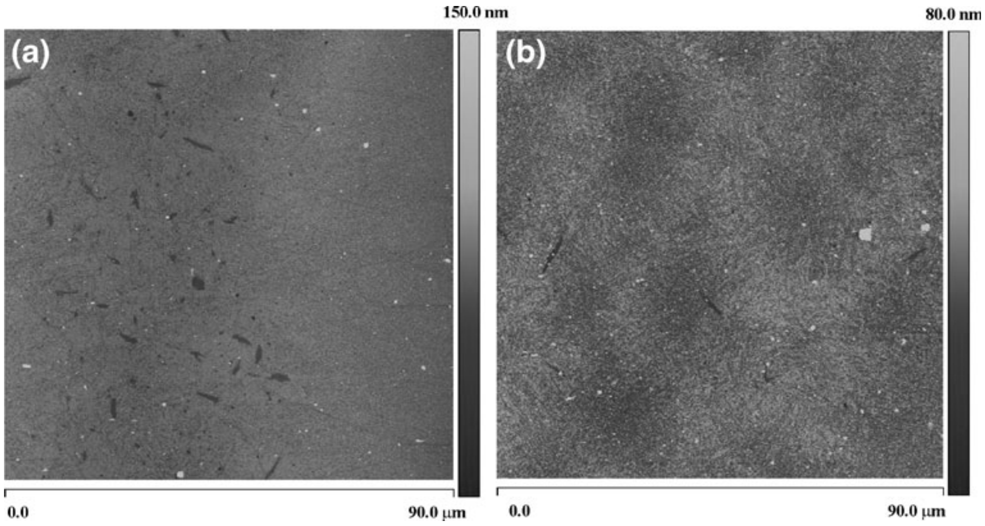

Fig. 3 Two AFM images taken from the shutter component with 480 nm-thick ITO bottom electrode, 230 nm-thick VO_2 film, and 160 nm-thick top ITO electrode after annealing the sample 20 min at the temperature of 450°C in a N_2 atmosphere. (**a**) Surface structure of the VO_2 layer and (**b**) surface structure of upper ITO layer

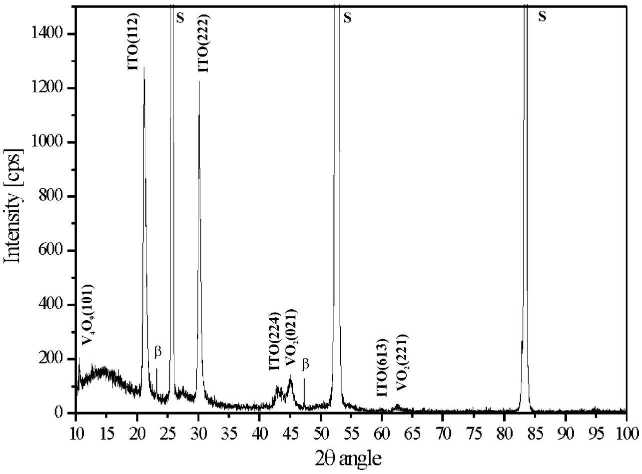

Fig. 4 XRD pattern measured from the two-layer shutter component with film thicknesses of 220 nm for bottom ITO electrode and 300 nm for VO_2 film. Substrate K_α and K_β reflections are labelled with S and β

in a N_2 atmosphere at the temperature of 300°C, and the uppermost pattern after annealing the sample 20 min in a N_2 atmosphere at the temperature of 450°C. The thicknesses of the layers were 480 nm for the bottom ITO electrode, 230 nm for the VO_2 film, and 160 nm for the top ITO electrode. It can be seen from the x-ray data that ITO layers of the component were polycrystalline with (112) and (222) as the main orientations with smaller (224), (441), (226), and (613) reflections. VO_2 film had polycrystalline crystal structure with (011), (002), (021), (220), and (221) crystal orientations. There was also a small amount of V_4O_9 and V_6O_{13} phases present in the structure of the VO_2 film. Secondary grain growth of VO_2 took place in the thin film during post-annealing, as can be seen from VO_2 (002), (020), and (220) peaks. Also, the splitting of ITO (112) and (224) peaks was reduced during the annealing process, which indicates the relaxation of the rather large residual strain originally present in the thin film structure.

Figure 3 presents two AFM images taken from the same three-layer shutter component as the XRD patterns of Fig. 2 were measured. AFM images are taken after annealing the sample 20 min in a N_2 atmosphere at the temperature of 450°C. The image in Fig. 3(a) was taken from the surface of the vanadium oxide layer and Fig. 3(b) presents the surface structure of the top ITO layer. These images and a higher resolution AFM image taken from the VO_2 and top ITO layers showed that some shallow cracking has taken place due to stress relaxation. The bottom ITO electrode layer was, however, intact and very smooth with a root mean square surface roughness (R_q) value of 1.26 nm and average surface roughness (R_a) value of 0.96 nm. Corresponding R_q and R_a values for the top ITO electrode were 19.7 nm and 7.26 nm and for the VO_2 layer 11.4 nm and 6.53 nm.

An x-ray diffraction pattern which was measured from the two-layer shutter component with a 220 nm-thick bottom electrode ITO layer and 300 nm-thick vanadium dioxide layer is presented in Fig. 4. Two AFM surface images taken from the same component are presented in Fig. 5. The XRD pattern shows that the ITO thin film was polycrystalline with (112) and (222) crystal orientations with minor reflections from (224) and (613) planes. The VO_2 film was composed of only (021) and (221) orientations and a small amount of the V_4O_9 phase. AFM image Fig. 5(a) was taken on the surface of the VO_2 layer, and it was found that also in this case some shallow cracking of the film has taken place. However, cracking of the two-layer components is far less severe than in the case of the three-layer structure. As in the case of the three-layer shutter component, the bottom ITO layer of the two-layer design was very flat with R_q=1.83 nm and R_a=0.486 nm. The vanadium oxide layer had R_q=14.9 nm and R_a= 7.95 nm, respectively. In the case of the two-layer component, no post-annealing was needed. This is most probably due to a thicker VO_2layer, which makes it

Fig. 5 Two AFM surface images taken from the two-layer shutter component with layer thicknesses of 220 nm for the bottom electrode ITO layer and 300 nm for the VO_2 layer. VO_2 film (**a**) and bottom ITO electrode (**b**)

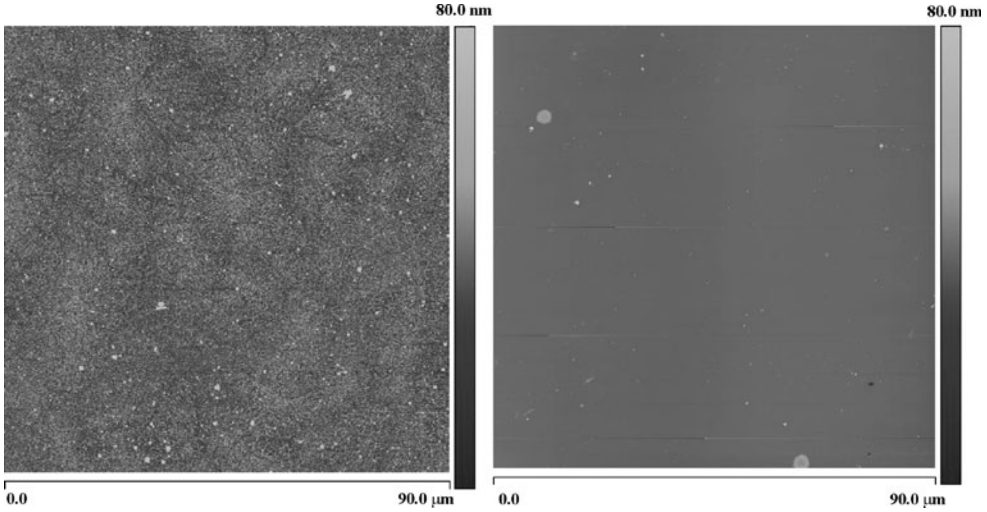

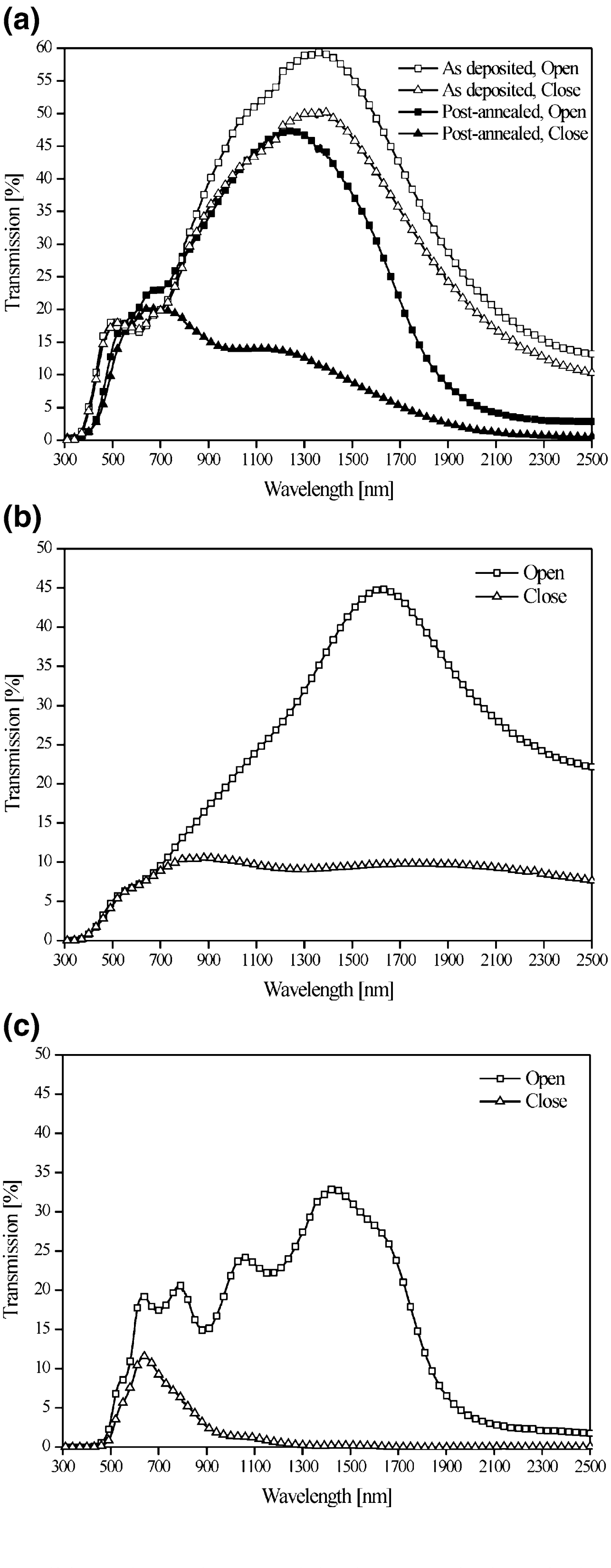

◀**Fig. 6** Optical transmittance spectra of three-layer shutter component after in-situ deposition and after annealing for 20 min at the temperature of 450°C in the N_2 atmosphere (**a**), two-layer shutter component (**b**), and the unoptimized three-layer component (**c**) with 650 nm-thick bottom ITO layer, 240 nm-thick VO_2 layer, and 650 nm-thick upper ITO layer

possible for internal stress originating from the large lattice mismatch between the ITO and VO_2 films to relax as the function of film thickness. Also in the two-layer component structure the vanadium dioxide film is clamped only from one side by the ITO film which will significantly reduce the strain and cracking of the VO_2 film.

Optical transmittance spectra measured from the two IR-shutters are presented in Fig. 6. Both spectra of the components in open state and in closed state after the MIT of the VO_2 film has taken place are shown. In both component designs, the limiting factor of the optical transmittance at the wavelengths above 1900 nm was the transmittance of ITO films.

Data from Fig. 6(a) was measured from the three-layer shutter component after annealing the component 20 min at the temperature of 450°C in a N_2 atmosphere. In the case of all the produced three-layer components, the optical response measured right after deposition was found to be rather poor. This is mainly due to large strain inside the thin film stack, which resisted the phase transition of the VO_2. When samples were post-annealed in the furnace, the magnitude of the change of the optical transmittance during the MIT was increased when the internal stress was relaxed. However, when the optical modulation increased, the optical transmittance value of the components in open state decreased. This is most probably due to microstructure evolution of the thin films of the multilayer structure during the annealing process. The transmittance maxima of components with three-layer structure was also shifted towards the lower wavelengths from the originally designed

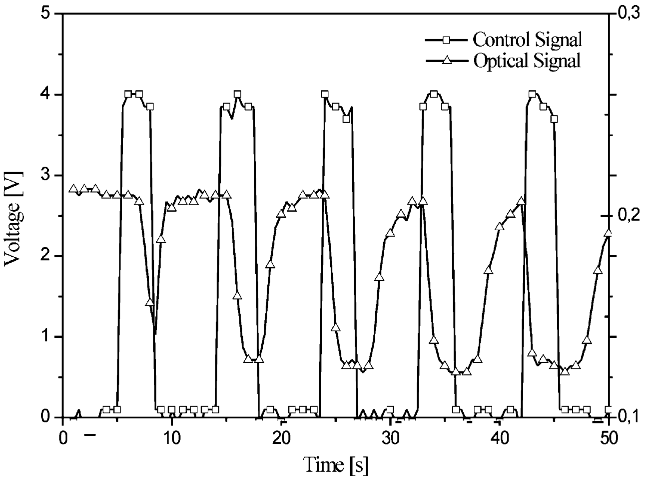

Fig. 7 Dynamic response measured from the three-layer shutter component combined with the control signal. The voltage was switched between 0 and 4 volts. The pulse duration was 3 s and duty cycle 33%

wavelength of 1550 nm and was typically placed between the wavelengths of 1100 and 1300 nm. The reason for this change is most probably the deviation of the thicknesses of deposited films from the calculated film thickness values and the fact that the deposited VO_2 films also contained other vanadium oxide phases which changed the refraction index of the deposited films from the index values used in theoretical calculations. The change of optical transmittance at the wavelength of 1550 nm during the switch cycle between open and closed states presented in Fig. 6(a) was 26.5%. The maximum modulation value was reached at the wavelength of 1250 nm and it was 34%. Spectra from Fig. 6(b) are measured from the two-layer component. From this optical data, it can be seen that interference maxima was placed very precisely around the wavelength of 1550 nm. Also the magnitude of the optical transition was larger than in the case of the three-layer design. The change of optical transmittance at this wavelength was found to be 34.2%. Figure 6(c) presents the optical response of the unoptimized three-layer shutter component with a 650 nm bottom ITO layer, 240 nm-thick VO_2 layer, and 650 nm upper ITO layer. The change of optical transmittance at the wavelength of 1550 nm was 29.5%. The modulation maximum was shifted to the wavelength of 1430 nm and it was 32.9%. Figure 7 presents the dynamic response combined with the control signal measured from the three-layer IR-shutter. The shutter was driven by a 4 V voltage pulse with a pulse duration of 3 s and duty cycle of 33%. Because of the large thermal masses of the components, the operation speed in both component designs was less than 1 Hz. The full reversibility of the metal-insulator transition of VO_2 can clearly be seen from this data.

4 Conclusion

IR-shutter components based on the ITO-VO_2 thin film stack with two different designs were produced by using the PLD method and their structural and optical characteristics were evaluated. In the case of the three-layer design, the XRD analysis showed that all the deposited ITO and VO_2 films of the components had polycrystalline crystal structure. The XRD analysis also gave some indication of the presence of other vanadium oxides in the VO_2 film. The strong residual strain originating from the large lattice mismatch between the ITO and VO_2 resisted the phase transition of the vanadium dioxide films. To relax the strain, the components were post-annealed in the N_2 atmosphere. The relaxation of internal stress led to the microstructure evolution of the thin films, which deteriorated the optical performance of the shutter components. The maximum change of the optical transmittance measured from the three-layer components during the switch cycle at the wavelength of 1550 nm was 26.5%.

In the case of the two-layer shutter design, the XRD analysis showed that the deposited ITO and VO_2films had a very similar crystal structure to that in the case of the three-layer design. In the case of the two-layer design, the strain between the thin films was not a problem and no post-annealing of the components was needed. The largest modulation of optical transmittance measured from the two-layer shutter component at the wavelength of 1550 nm was 34.2%. Because of the large thermal masses, the switching speed of the components was rather slow. However, the measurements clearly showed that the MIT of VO_2 is fully reversible. The performance of the shutter component could be enhanced by further optimizing the thin film deposition process to eliminate the unwanted vanadium oxide phases from the VO_2 film. Also, other electrode materials could be considered and new component design with a smaller thermal mass could be used to increase the operation speed of the shutter.

This research was part of the NAPERO (Development of novel fabrication methods for nanoscale photonics and microelectronics components) project, funded by TEKES (National Technology Agency of Finland). Research was carried out in co-operation with the Micro–and Nanotechnology Center (MNT) of the University of Oulu.

References

1. F.J. Morin, Phys. Rev. Lett. **3**, 34 (1959)
2. M. Gupta, A.J. Freeman, D.E. Ellis, Phys. Rev. B **16**, 3338 (1977)
3. J. Lappalainen, S. Heinilehto, S. Saukko, V. Lantto, H. Jantunen, Sensor Actuat. A-Phys. **142**, 250–255 (2008)
4. P. Jin, S. Tanemura, Jpn. J. Appl. Phys. **33**, 1478 (1994)
5. A.A. Velichko, N.A. Kuldin, G.B. Stefanovich, A.L. Pergament, Tech. Phys. Lett. **29**, 507 (2003)
6. H. Wang, X. Yi, S. Chen, X. Fu, Sensor Actuat. A-Phys. **122**, 108 (2005)
7. D. Xiao, K.W. Kim, J.M. Zavada, J. Appl. Phys. **97**, 1 (2005)
8. C.-A. Nguyen, H.-J. Shin, K.T. Kim, Y.-H. Han, S. Moon, Sensor Actuat. A-Phys. **123**, 78 (2005)
9. M.-H. Lee, M.-G. Kim, Thin Solid Films **286**, 219 (1996)
10. C. Jinzhong, D. Daoan, J. Wanshun, Appl. Surf. Sci. **133**, 225 (1998)
11. M. Nagashima, H. Wada, K. Tanikawa, H. Shirahata, Jpn. J. Appl. Phys. **37**, 4433 (1998)
12. Y. Muraoka, Z. Hiroi, Appl. Phys. Lett. **80**, 4 (2002)
13. F. Béteille, L. Mazerolles, J. Livage, Mater. Res. Bull. **3**, 2177 (1999)
14. F.O. Adurodija, H. Izumi, T. Ishihara, H. Yoshioka, H. Matsui, M. Motoyama, Vacuum **59**, 641 (2000)
15. T. Wittkowski, J. Jorzick, H. Seitz, B. Schröder, K. Jung, B. Hillebrands, Thin Solid Films **398–399**, 465 (2001)
16. S.H. Kim, N.-M. Park, T.Y. Kim, G.Y. Sung, Thin Solid Films **475**, 262 (2005)